Automatic Solar Photovoltaic Panel Detection in Satellite Imagery

Jordan M. Malof, Rui Hou, Leslie M. Collins
Electrical and Computer Engineering
Duke University
Durham, NC, USA
jmmalo03@gmail.com

Kyle Bradbury, Richard Newell
Duke University Energy Initiative
Duke University
Durham, NC, USA
kyle.bradbury@duke.edu

Abstract—**The quantity of rooftop solar photovoltaic (PV) installations has grown rapidly in the US in recent years. There is a strong interest among decision makers in obtaining high quality information about rooftop PV, such as the locations, power capacity, and energy production of existing rooftop PV installations. Solar PV installations are typically connected directly to local power distribution grids, and therefore it is important for the reliable integration of solar energy to have information at high geospatial resolutions: by county, zip code, or even by neighborhood. Unfortunately, traditional means of obtaining this information, such as surveys and utility interconnection filings, are limited in availability and geospatial resolution. In this work a new approach is investigated where a computer vision algorithm is used to detect rooftop PV installations in high resolution color satellite imagery and aerial photography. It may then be possible to use the identified PV images to estimate power capacity and energy production for each array of panels, yielding a fast, scalable, and inexpensive method to obtain rooftop PV estimates for regions of any size. The aim of this work is to investigate the feasibility of the first step of the proposed approach: detecting rooftop PV in satellite imagery. Towards this goal, a collection of satellite rooftop images is used to develop and evaluate a detection algorithm. The results show excellent detection performance on the testing dataset and that, with further development, the proposed approach may be an effective solution for fast and scalable rooftop PV information collection.**

Keywords-component; detection, solar, energy, photovoltaic

I. INTRODUCTION

The quantity of rooftop solar photovoltaic (PV) installations has grown rapidly in the US in recent years [1], [2]. Although there are many environmental and economic benefits from solar energy, effectively integrating rooftop PV into existing power grids presents many challenges. In contrast to traditional forms of energy generation, such as coal and natural gas, rooftop PV is a distributed energy source and generates power intermittently, dependent on solar insolation. To aid in PV integration there is strong interest among government and utility decision-makers in obtaining detailed information about rooftop PV, such as the locations, capacity, and energy production of existing rooftop PV installations. This information is useful for important decisions such as energy policy and regulation; system planning for capacity expansion, transmission and distribution upgrades; and for operations decisions to ensure grid reliability and resilience.

As a further challenge, the aforementioned decisions must be made for localized geographic regions like towns and counties (rather than states), necessitating that the corresponding rooftop PV information be geospatially precise. Unfortunately, traditional means of obtaining energy information is poorly suited for this purpose. Traditional methods, such as surveys and utility company interconnection filings, are burdensome and yield insufficient amounts of data for the desired geospatial precision. Further, due to the rapid growth of rooftop PV, any such estimates quickly become outdated; requiring regularly conducted, and often expensive, data collections. These challenges motivate the search for a new approach to obtain rooftop PV information.

In this work a new approach to obtain rooftop PV information is investigated where individual rooftop PV panels are automatically identified in high resolution color satellite imagery. It is impractical for humans to visually scan the necessary volumes of data for this solution, but it may be possible for a computer algorithm to do so. If rooftop PV can be reliably identified by computers then PV information, potentially including their capacity and energy generation, can be quickly estimated at almost any level of geospatial precision. This approach could therefore potentially yield a fast, reliable, and scalable way to obtain rooftop PV information.

The aim of this work is to perform experiments to investigate the feasibility of this new energy information data mining approach. A rooftop PV detection algorithm was developed and its effectiveness was evaluated on a collection of rooftop satellite imagery available from the US Geological Survey [3]. The results show that excellent detection performance can be obtained on the test dataset (94% of 53 panels detected, with only 4 false detections). This indicates that, with further development, the proposed approach may be an excellent method for obtaining distributed PV energy information.

The remainder of this paper is organized as follows. Section II describes the experimental color satellite orthoimagery dataset. Section III presents the rooftop PV detection algorithm. Section IV describes the experimental design and the results of the detection algorithm on the dataset. Finally, Section V presents our conclusions and ideas for future work.

II.   COLOR SATELLITE IMAGERY DATASET

The experimental data used in this work consisted of house images extracted from publicly available satellite orthoimagery obtained from the U.S. Geological Survey (USGS). The imagery was collected over the city of Lemoore, CA during 2014 at a resolution of 0.3m, and with 8-bit resolution in each color channel. From this imagery a total of 100 different houses were manually selected for inclusion in the dataset. The first 50 houses were chosen so that they each contained one or more rooftop PV installations. The second 50 houses were chosen because they did not contain a PV installation. A rectangular region of the image data was extracted around each house, containing the house rooftop and some surrounding area. The collection of all the house images corresponds to a total surface area of 0.196 km^2. For algorithm training and scoring, a human annotator manually drew polygons around all rooftop PV installations in each of the images. Some images from the resulting dataset, along with some rooftop PV annotations (black polygons), are shown in Fig. 1.

III.   ROOftop PV detection algorithm

This section presents a computer vision algorithm that was developed with the goal of detecting rooftop PV installations in the experimental dataset described in Section II. The algorithm takes an image as input and returns a set of regions (each region being a group of pixels) and a decision statistic, or confidence, for each region indicating how likely that region is to be a rooftop PV installation. This processing chain is illustrated in Fig. 2.

The algorithm consists of two different stages: prescreening and feature processing. The goal of prescreening is to reduce the number of image locations that must be considered for feature processing, which is more computationally expensive and would be prohibitively slow if all pixels in the images were considered individually. The prescreener also groups pixels into regions so that features may be computed on regions rather than individual pixels. This can aid in computing features such as shape and texture. Similar approaches that group pixels into regions have been used successfully in recent object detection studies with satellite imagery[4]–[6]. The prescreener operates by converting an image from RGB to grayscale and identifying all Maximally Stable Extremal Regions (MSERs) in the image [7], within certain size constraints. The resulting set of regions is then reduced by removing the 30% of regions with the lowest prescreener confidence values, denoted c, where c is given by

$$c = \log \Pr(X_{region}|M_{PVRGB}).   (1)$$

Here X_{region} is the (3-dimensional) mean RGB value in each detected region, and M_{PVRGB} denotes a multivariate normal probability distribution with mean and covariance parameters that were inferred from the hand annotated truth regions. The model parameters were inferred using the entire dataset (including testing data), which may introduce a positive bias to the detection performance, however we do not believe this bias will be large because the model is very simple.
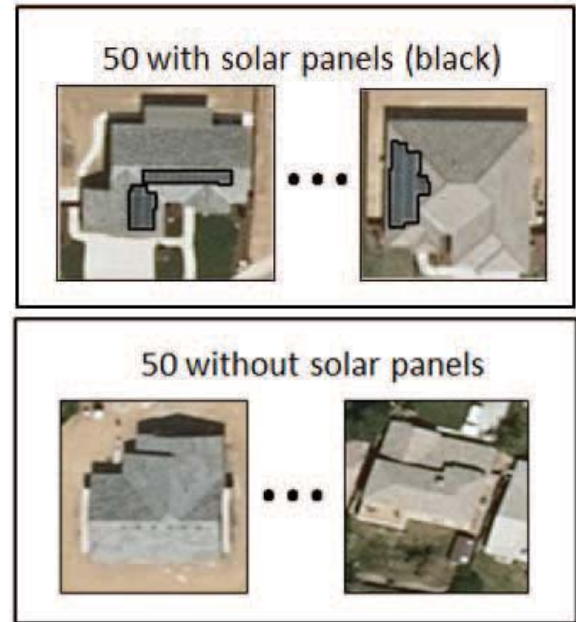

Fig. 1 Experimental dataset of satellite suburban house images. This figure illustrates the structure of the experimental dataset for the work presented in this paper. The dataset consists of 100 satellite images over rooftops in a suburb of Lemoore, California. Half of the images were collected over houses with one, or more, rooftop PV installations (top panel). The other half of the images were collected over houses without any rooftop PV installations (bottom panel). A human annotator drew polygons around each individual rooftop PV installation in the images (black polygons in top panel).
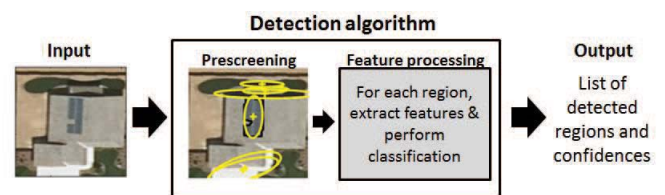

Fig. 2 Detection algorithm overview. This figure illustrates the general operation of the rooftop PV detection algorithm. The input to the algorithm is a color satellite image (left-most image). The algorithm first applies a prescreening operation that identifies regions (yellow ellipses in middle-left image) which are then considered for more sophisticated feature processing (middle-right image). Features are extracted from each region and then a trained support vector machine classifier is used to classify the features. The output of the algorithm is a list of regions and their respective confidence values, indicating how likely they are to correspond to a rooftop PV installation.

The next step of the detection algorithm is feature processing. Several features are extracted from each prescreener region, which are then used by a machine learning classifier to assign a new decision statistic to the region. The features used for classification are summarized below in Table I. These features are based on standard features that can be found in many computer vision textbooks [8], [9]. Once features are extracted, a support vector machine (SVM) classifier, with a radial basis function kernel, is used to classify each of the regions based on their features. Several other classifiers were also considered but the SVM performed best. The final result of the detection algorithm is a list of regions, each having a decision statistic that was assigned by the SVM classifier. As a final post-processing step, the mean-shift clustering algorithm [10], [11] is used to combine any regions that are located very close to one another, and therefore might correspond to the same object. A Gaussian kernel was used with a spatial bandwidth of 5 pixels (1.5 meters). If multiple detections are clustered together, then the detection with the highest classifier confidence is retained to represent the cluster, and the other detections are discarded.

TABLE 1
FEATURES EXTRACTED FROM EACH REGION DETECTED BY THE PRESCREENER.

Feature name	Feature description	Feature Space Dimensionality
Foreground color	Prescreener confidence, c see eq. (1)	1
Background color	First 10 principal components of 3-D color histogram of background pixels	10
Shape features 1	Perimeter length, Extent = Area/BoundingBoxArea	2
Shape features 2	Compactness = Area/Perimeter^2, Solidity = Area/BoundingArea	2
Texture features	Mean, Variance, and Kurtosis of grayscale pixels within region	3

IV. EXPERIMENTAL DESIGN AND RESULTS

This section presents the experimental results obtained by testing the rooftop PV algorithm described in Section III using the rooftop PV dataset described in Section II. Performance was evaluated using receiver operating characteristic (ROC) curve analysis on the confidence values assigned to the regions detected by the algorithm.

In addition to a confidence value, to perform ROC analysis, each detected region must be assigned either as a correct detection or a false detection. There are many ways of making this assignment. The primary goal of the rooftop PV algorithm developed in this work was to count solar panels (as opposed to quantify panel area) and so a rule was designed to best quantify the ability of the algorithm to perform this task. One challenge for designing this rule was that many detected regions were completely, or largely, located within an annotated rooftop PV region, but did not cover a large portion of that truth region. A few examples can be seen in Fig. 4 below (bottom left-most images). Therefore, a detected region was considered a hit if at least 50% of the detected region was

within the annotated truth region, and at least 10% of the human annotation was within the detected region. All detected regions that did not fit these two criteria were considered false detections.

The ROC curve for the prescreener was obtained by thresholding the prescreener confidences, denoted c in (1), assigned to each false detection region, and each region that was a correct detection. This ROC curve is displayed with the red solid line in Fig. 3. The x-axis shows the false detections per square kilometer of image area. The y-axis shows the proportion of targets detected. The results show that the prescreener detects up to 94% of the targets if the allowed number of false detections is increased. Note that this limits the feature processing stage to detecting, at most, 94% of the targets as well. At a detection rate of 94% the prescreener yields roughly 175 false detections per km^2, which corresponds to about 34 false detections over the entire dataset. It is the goal of the feature processing stage to reduce the number of false detections while still maintaining most, or all, of the correct detections.

The ROC curve for the feature processing stage was obtained by employing a leave-one-image-out cross-validation scheme for training and testing the SVM classifier and features described in Section III. More specifically, the cross-validation procedure consisted of 100 training-testing cycles. In each cycle a single image is used for testing and the remaining 99 are used for training the SVM classifier on features extracted from the prescreener regions from those 99 training images. The trained classifier was then used to classify (i.e., assign confidences to) the prescreener regions detected in the test image. This process was repeated 100 times until each image had been in the testing set exactly once. The ROC curve for the feature processing stage is displayed with the dashed black line in Fig. 3. From the results it is clear
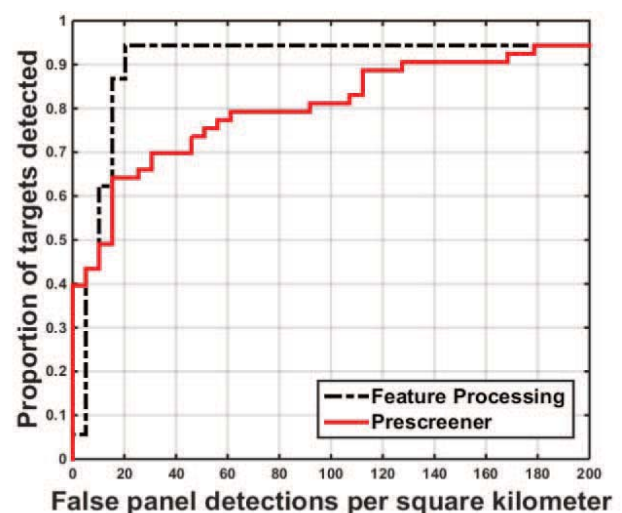

Fig. 3 ROC curve for the rooftop PV detection algorithm. This figure shows the receiver operating characteristic (ROC) curve for the prescreener (solid red) and the feature processing (dashed black) for the rooftop PV detection algorithm. The feature processing algorithm can detect 94% of true panels at a false detection rate of 20 FA/km^2 (only 4 false detections in the dataset).

that the feature processing substantially improves over the prescreener, obtaining 94% of the targets with a much lower false detection rate of 20 false detections per km^2. This corresponds to about 4 false detections over the entire dataset.

Fig. 4 shows several house images and the resulting detected regions if the detector is operated with a 94% correct detection rate. The human annotations are shown in black and the detected regions are indicated with yellow ellipses. It should be noted that the regions detected by the algorithm are not actually elliptical. The ellipses are proportional in size and orientation to the detected regions, and are used to aid with visualization. The results show that the detector is capable of identifying PV panels in a variety of shapes and sizes, although sometimes the detected regions are much smaller than the true rooftop PV installation (see bottom left-most images).

Fig. 4 Example results from the rooftop PV detection algorithm. This figure shows 15 examples of the satellite images input to the rooftop PV detection algorithm for testing, along with the human annotated rooftop PV installations (black) and the regions detected by the rooftop PV detection algorithm (yellow ellipses). The actual output of the algorithm is a list of pixels and the yellow ellipses are used for ease of visualization. The ellipses are proportional to the size and orientation of the detected regions. In these images all the true rooftop PV installations were detected by the algorithm except for one (top right). The set of detected regions shown here was obtained by including only regions with a confidence above a threshold. The threshold corresponds to an operating point on the ROC curve (Fig. 3) of a detection rate of 94%.

V. CONCLUSIONS

In this work a new approach for collecting energy information for rooftop PV was investigated. This approach involves using computer algorithms to automatically identify rooftop PV installations in high resolution (0.3m per pixel) color satellite orthoimagery. The specific goal of this work was to explore the feasibility of this approach for further research and development. To achieve this goal a dataset of 100 images from the U.S. Geological Survey was gathered for experiments. Human annotators manually drew polygons around all of the rooftop PV installations in the imagery (53 installations in total). A computer vision algorithm was developed to detect rooftop PV installations, and its performance was measured on the dataset using ROC analysis. The results show that the algorithm can achieve a correct detection rate of 94% (i.e., 50 of 53 PV installations detected) with only 4 false detections. This suggests that, with further development, this approach could offer a new automatic, fast, and scalable approach to obtaining rooftop PV information. Future work will focus on further improving the detection performance of the rooftop PV detection algorithm, and ensuring that its performance is consistent across many different landscapes.

REFERENCES

[1] M. J. E. Alam, K. M. Muttaqi, and D. Sutanto, "An approach for online assessment of rooftop solar PV impacts on low-voltage distribution networks," *IEEE Trans. Sustain. Energy*, vol. 5, no. 2, pp. 663–672, 2014.

[2] A. Chersin, W. Ongsakul, J. Mitra, and S. Member, "Improving of Uncertain Power Generation of Rooftop Solar PV Using Battery Storage," in *International Conference and Utility Exhibition on Green Energy for Sustainable Development*, 2014, March, pp. 1–4.

[3] "US Geological Survey High Resolution Orthoimagery," *US Geological Survey Website*, 2015. [Online]. Available: http://cumulus.cr.usgs.gov/listofortho.php.

[4] J. Graesser, A. Cheriyadat, R. R. Vatsavai, V. Chandola, J. Long, and E. Bright, "Image based characterization of formal and informal neighborhoods in an urban landscape," *IEEE J. Sel. Top. Appl. Earth Obs. Remote Sens.*, vol. 5, no. 4, pp. 1164–1176, 2012.

[5] S. W. Myint, P. Gober, A. Brazel, S. Grossman-Clarke, and Q. Weng, "Per-pixel vs. object-based classification of urban land cover extraction using high spatial resolution imagery," *Remote Sens. Environ.*, vol. 115, no. 5, pp. 1145–1161, 2011.

[6] K. R. Varshney, G. H. Chen, B. Abelson, K. Nowocin, V. Sakhrani, L. Xu, and B. L. Spatocco, "Targeting Villages for Rural Development Using Satellite Image Analysis," *Big Data*, vol. 3, no. 1, pp. 41–53, 2015.

[7] J. Matas, O. Chum, M. Urban, and T. Pajdla, "Robust wide-baseline stereo from maximally stable extremal regions," *Image Vis. Comput.*, vol. 22, no. 10, pp. 761–767, Sep. 2004.

[8] R. Szeliski, *Computer Vision : Algorithms and Applications*. Springer, 2010.

[9] D. Forsyth and J. Ponce, *Computer vision: a modern approach*, 2nd ed. Pearson, 2012.

[10] K. Fukunaga and L. Hostetler, "The Estimation of the Gradient of a Density Function , with Applications in Pattern - Recognition," *Inf. Theory, IEEE ...*, vol. lim, no. 4, pp. 32–40, 1975.

[11] D. Comaniciu, P. Meer, and S. Member, "Mean Shift : A Robust Approach Toward Feature Space Analysis," *... Anal. Mach. Intell. ...*, vol. 24, no. 5, pp. 603–619, 2002.